Journal of Magnetism and Magnetic Materials 394 (2015) 179–184

Contents lists available at ScienceDirect

Journal of Magnetism and Magnetic Materials

journal homepage: www.elsevier.com/locate/jmmm

A study on the origin of room temperature ferromagnetism in $Ni_{1-x}Gd_xO$ nanoparticles

B. Gokul [a], P. Saravanan [b], V.T.P. Vinod [c], Miroslav Černík [c], R. Sathyamoorthy [a],*

[a] PG and Research Department of Physics, Kongunadu Arts and Science College (Autonomous), Coimbatore 641029, India
[b] Defence Metallurgical Research Laboratory, Kanchanbagh, Hyderabad 500058, India
[c] Institute for Nanomaterials, Advanced Technologies and Innovation, Department of Natural Sciences, Technical University of Liberec, Studentská 1402/2, Liberec 1, 461 17 Czech Republic

ARTICLE INFO

Article history:
Received 23 May 2015
Accepted 23 June 2015
Available online 25 June 2015

Keywords:
Hydro-thermal synthesis
Nickel oxide nanoparticles
Room-temperature ferromagnetism
Diluted magnetic semiconductors.

ABSTRACT

We herein report the existence of room temperature (RT) ferromagnetism (FM) in Gd-doped NiO nanoparticles prepared by hydrothermal process. The Gd-content in $Ni_{1-x}Gd_xO$ was varied from 0.01 to 0.1 and the resultant structural and magnetic properties due to Gd-doping were studied using X-ray diffraction (XRD), transmission electron microscopy (TEM), micro- Raman spectroscopy and vibrating sample magnetometer (VSM). The composition analysis and charge state were obtained from energy dispersive x-ray spectroscopy (EDS) and x-ray photoelectron spectroscopy (XPS), respectively. Both pure and Gd-doped NiO nanoparticles retained face centered cubic crystal structure. Formation of any secondary phases or metallic clusters related to pure Gd or Ni is not evident in the as-synthesized samples. TEM analysis revealed that the particles are spherical with sizes in the range of 8 – 18 nm. Micro-Raman spectra showed increase in Ni-vacancies with increase of Gd-concentration. XPS spectra of Gd-doped NiO revealed a shift in binding energy compared to the pure NiO, implies the replacement of Gd atoms in Ni-vacancies. Interesting RT-FM behavior is observed for the Gd concentrations of 7 and 10%; while the pure NiO and the other lower concentrations of Gd-doping demonstrated paramagnetic nature. The observed RT-FM can be attributed to the Ni vacancies induced by the doping of Gd^{3+} ions and this fact is explained on the basis of bound magnetic polaron model.

1. Introduction

Modern micro-magnetic/electronic devices mainly exploit the synergetic properties of both charge and spin of the electrons (spintronics). Over the past two decades, there has been a technological revolution in generating, manipulating, detecting and injecting spin-polarized carriers into non-magnetic semiconductors towards realizing the potential benefits of spintronic devices. Dilute magnetic semiconductor (DMS) materials are potential candidates for the spin-polarized devices such as magneto-optical, spin-based sensors and other logical devices [1]. Semiconductor metal oxides such as ZnO, TiO_2 and SnO_2 have been often doped with magnetic transition metal ions or rare earth ions in order to have dilute ferromagnetism and Curie temperatures (T_c) of >300 K [2]. Such doped metal oxides are wide band gap semiconductors having *n*-type electrical conduction. Nevertheless, the spin based electronic devices, viz., spin LEDs and spin sensors mostly demand *p*-type DMS to form an effective *p*–*n* junction [3]. To achieve *p*-type conduction in such transition metal oxide semiconductors is a major challenge to the scientific community [4].

At RT, stoichiometric nickel oxide (NiO) is a Mott-Hubbard insulator with resistivity of about $10^{13}\ \Omega$ cm [5]. With Ni^{2+} ion vacancies, NiO is a *p*-type semiconductor with band gap varying from 3.6 to 4 eV [6] and has been employed as an active layer in dye sensitized solar cells, Ni-ion batteries and also, as an antiferromagnetic (AFM) layer in spin-valve structures, resistive and magnetoresistive memory devices. In addition, NiO can find applications in smart windows and electrochemical super-capacitors owing to its interesting electrochromic property [7]. NiO crystallizes in a face centered cubic structure (FCC) with space group of $Fm\bar{3}m$. When NiO is doped with Fe and Mn, it shows properties of dilute magnetic and semiconductor [8]; while Li co-doped with 3*d* transition metal ions such as Fe, V and Mn in NiO thin films showed enhanced ferromagnetism at RT [9]. Recent theoretical and experimental studies revealed that by doping rare-earth (RE) metal ions with metal oxide semiconductors, high T_c in DMS

---

* Corresponding author.
E-mail address: rsathya59@gmail.com (R. Sathyamoorthy).

http://dx.doi.org/10.1016/j.jmmm.2015.06.060
0304-8853/© 2015 Elsevier B.V. All rights reserved.

materials could be achieved [10]. RE metal ions like Gd, Nd, etc., have been already reported to exhibit RT-FM with giant magnetic moment [11]. In particular, Gd-doped GaN DMS have shown extraordinary magnetic moments up to 4000 μ_B and T_c of above 300 K [12]. This unusual high magnetic moment is attributed to the partially filled 4*f* orbital of Gd; whereas in the case of transition metals like Mn, Fe and Co, the 3*d* electrons are delocalized and hence, they tend to offer feeble magnetic moments due to low orbital momentum [13,14]. In view of the above, we herein intend to dope Gd with AFM–NiO for the benefit of imparting RT-FM. The influence of Gd-concentration on the structural and magnetic properties of NiO nanoparticles was investigated and the existence of RT-FM is explained based on the bound magnetic polaron (BMP) mechanism.

2. Experimental details

2.1. Synthesis of $Ni_{1-x}Gd_xO$ nanoparticles

$Ni_{1-x}Gd_xO$ (x=0.01, 0.025, 0.05, 0.075 and 0.1) nanoparticles were prepared by hydrothermal process. $Ni(NO_3)_2 \cdot 6H_2O$, $Gd(NO_3)_2 \cdot 3H_2O$ and urea were used as precursors and complexing agent, respectively. 0.1 M of $Ni(NO_3)_2 \cdot 6H_2O$ and appropriate amount of $Gd(NO_3)_2 \cdot 3H_2O$ were dissolved in 30 mL of deionized water and the resultant solution was stirred for 30 min to obtain a homogenous solution. 0.3 M Of urea was then added to the cationic precursor solution under continuous stirring. The solution was transferred to a Teflon-lined stainless steel autoclave and heated to a temperature of 180 °C for 6 h. The resultant precipitates were washed several times with deionized water and ethanol. The precipitates were finally dried in a hot air oven at 100 °C and the dried powders were further subjected to annealing at 300 °C for 3 h.

2.2. Characterization of $Ni_{1-x}Gd_xO$ nanoparticles

The phase composition of Gd-doped NiO nanoparticles was studied by Shimadzu -XRD-6000 X-ray diffractometer using Cu-K_α radiation (λ=1.54060 Å) with a scanning rate of 0.02 °/s. The morphology of NiO nanoparticles was observed using a JEOL-JEM 2100 transmission electron microscopy (TEM). Raman spectra was obtained from Renishaw Invia Reflex micro Raman spectrometer at 514 nm laser excitation of Ar laser with a spectral resolution, i.e full-width half-maximum, FWHM of 1 cm^{-1}. Oxidation state of Gd-doped NiO nanoparticles was identified using Kratos Analytical Axis Ultra DLD with Al Ka1 source with energy of 1.486 keV. Magnetic measurements were carried out using Lakeshore vibrating sample magnetometer (Model VSM-7410).

3. Results and discussion

3.1. Structural and morphological study

In Fig. 1a, we show the XRD patterns of $Ni_{1-x}Gd_xO$ nanoparticles synthesized with different Gd concentrations. The diffraction peaks of both pure and Gd-doped NiO nanoparticles indicate the polycrystalline nature and are identified as fcc-structure of rock salt NiO with space group of $Fm\bar{3}m$. The lattice parameter (*a*) values were calculated and these values are found to increase from 4.179 to 4.193 Å with increase in Gd concentration. The diffraction peaks observed for the 2θ values of 37.3, 43.2, 62.9, 75.5 and 79.4° can be indexed to the reflections of (111), (200), (220), (311) and (222) with the standard JCPDS data (Card no. 78-0643). Impurity phases such as Gd_2O_3 are not evidenced in the XRD patterns. All the diffraction peaks show peak-broadening due to the nanocrystalline nature. In addition, it can be noticed that the intensity of the diffraction peaks decreases with the addition of Gd and the FWHM gets broadened. The predominant peak at 43.2° clearly shows a low angle shift due to the increase in Gd-concentration (Fig. 1b). This may be due to the diffusion of Gd atoms into the Ni-lattice [15]. The interplanar spacing increases with the Gd-concentration and higher concentration of Gd may cause compressive stress which results in lattice distortion [16]. This lattice distortion is due to the large difference in the ionic radius between Ni^{2+} (0.72 Å) and Gd^{3+} (0.938 Å), changes in the bond length, bond angles between the atoms [17]. The average crystallite size of Gd-doped NiO nanoparticles were estimated using Debye-Scherrer's formula,

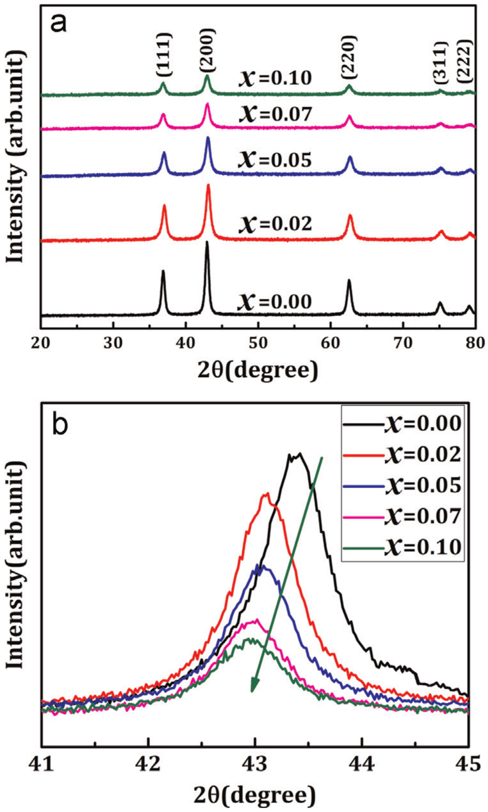

Fig. 1. X-ray diffraction patterns of $Ni_{1-x}Gd_xO$ (x=0.00, 0.02, 0.05, 0.07 and 0.10) nanoparticles (a) and 2θ shift in (200) peak position as a function of Gd-concentration (b).

$$D = \frac{0.94\lambda}{\beta_{hkl} \cos\theta} \tag{1}$$

where D is the average crystallite size, β is the FWHM, and λ is the wavelength of X-rays used (0.15406 nm).

The TEM micrographs of $Ni_{1-x}Gd_xO$ nanoparticles are shown in Fig. 2a–c. The bare NiO nanoparticles possess a very thin sheet-like layered hexagonal structure with tiny pores. When 2% of Gd is doped with NiO, the layered structure transformed into tiny nanoparticles of size 18 nm. Upon further increasing the Gd-doping to 10%, the particles become very tiny, with sizes of approximately 8 nm. A typical selected area electron diffraction (SAED) pattern of $Ni_{0.93}Gd_{0.07}O$ nanoparticles is shown in Fig. 2d. The observed ring pattern is very much consistent with the (111), (200), (220) (311) and (222) planes of fcc-NiO and these SAED results are in good agreement with the XRD studies. The EDS spectra of $Ni_{0.93}Gd_{0.07}O$ nanoparticles shown in Fig. 2e, apparently reveal the presence of Ni, Gd and O elements with no other impurities.